

Assembly of Severe Acute Respiratory Syndrome Coronavirus RNA Packaging Signal into Virus-Like Particles Is Nucleocapsid Dependent

Ping-Kun Hsieh, Shin C. Chang, Chu-Chun Huang,
Ting-Ting Lee, Ching-Wen Hsiao, Yi-Hen Kou, I-Yin Chen,
Chung-Ke Chang, Tai-Huang Huang and Ming-Fu Chang
J. Virol. 2005, 79(22):13848. DOI:
10.1128/JVI.79.22.13848-13855.2005.

Updated information and services can be found at:
<http://jvi.asm.org/content/79/22/13848>

These include:

REFERENCES

This article cites 31 articles, 14 of which can be accessed free
at: <http://jvi.asm.org/content/79/22/13848#ref-list-1>

CONTENT ALERTS

Receive: RSS Feeds, eTOCs, free email alerts (when new
articles cite this article), [more»](#)

Information about commercial reprint orders: <http://journals.asm.org/site/misc/reprints.xhtml>
To subscribe to to another ASM Journal go to: <http://journals.asm.org/site/subscriptions/>

Assembly of Severe Acute Respiratory Syndrome Coronavirus RNA Packaging Signal into Virus-Like Particles Is Nucleocapsid Dependent

Ping-Kun Hsieh,¹ Shin C. Chang,² Chu-Chun Huang,¹ Ting-Ting Lee,¹ Ching-Wen Hsiao,² Yi-Hen Kou,² I-Yin Chen,¹ Chung-Ke Chang,³ Tai-Huang Huang,³ and Ming-Fu Chang^{1*}

Institute of Biochemistry and Molecular Biology,¹ and Institute of Microbiology,² National Taiwan University College of Medicine, Taipei, Taiwan, and Institute of Biomedical Sciences, Academia Sinica, Taipei, Taiwan³

Received 10 April 2005/Accepted 20 July 2005

The severe acute respiratory syndrome coronavirus (SARS-CoV) was recently identified as the etiology of SARS. The virus particle consists of four structural proteins: spike (S), small envelope (E), membrane (M), and nucleocapsid (N). Recognition of a specific sequence, termed the packaging signal (PS), by a virus N protein is often the first step in the assembly of viral RNA, but the molecular mechanisms involved in the assembly of SARS-CoV RNA are not clear. In this study, Vero E6 cells were cotransfected with plasmids encoding the four structural proteins of SARS-CoV. This generated virus-like particles (VLPs) of SARS-CoV that can be partially purified on a discontinuous sucrose gradient from the culture medium. The VLPs bearing all four of the structural proteins have a density of about 1.132 g/cm³. Western blot analysis of the culture medium from transfection experiments revealed that both E and M expressed alone could be released in sedimentable particles and that E and M proteins are likely to form VLPs when they are coexpressed. To examine the assembly of the viral genomic RNA, a plasmid representing the GFP-PS580 cDNA fragment encompassing the viral genomic RNA from nucleotides 19715 to 20294 inserted into the 3' noncoding region of the green fluorescent protein (GFP) gene was constructed and applied to the cotransfection experiments with the four structural proteins. The SARS-CoV VLPs thus produced were designated VLP(GFP-PS580). Expression of GFP was detected in Vero E6 cells infected with the VLP(GFP-PS580), indicating that GFP-PS580 RNA can be assembled into the VLPs. Nevertheless, when Vero E6 cells were infected with VLPs produced in the absence of the viral N protein, no green fluorescence was visualized. These results indicate that N protein has an essential role in the packaging of SARS-CoV RNA. A filter binding assay and competition analysis further demonstrated that the N-terminal and C-terminal regions of the SARS-CoV N protein each contain a binding activity specific to the viral RNA. Deletions that presumably disrupt the structure of the N-terminal domain diminished its RNA-binding activity. The GFP-PS-containing SARS-CoV VLPs are powerful tools for investigating the tissue tropism and pathogenesis of SARS-CoV.

An international outbreak of severe acute respiratory syndrome (SARS), an atypical pneumonia, spread through more than 30 countries and caused about 8,422 cases and 916 deaths worldwide from its emergence in mid-November 2002 until 7 August 2003 (30). A novel coronavirus SARS-coronavirus (CoV) that can be isolated from the SARS patients and from Vero E6 cells inoculated with clinical specimens was identified to be the causative agent of SARS (7, 14, 15). SARS-CoV is an enveloped, positive-sense single-stranded RNA virus that is approximately 30,000 nucleotides (nt) in length, with virus particles ranging from 80 to 120 nm in diameter. It is phylogenetically different from the three previously identified coronavirus serotypes, but electron microscopy of the viral particles revealed that its features are characteristic of coronaviruses (23). The virus particle consists of four structural proteins: spike (S), membrane (M), small envelope (E), and nucleocapsid (N) (19, 25, 26). S protein is a type I integral membrane glycoprotein that makes up the crown-like appearance of the

viral particle (23). Angiotensin-converting enzyme 2 and CD209L (L-SIGN) were proposed to be the receptors responsible for viral entry by binding of the viral S protein to the receptors on specific cell types (13, 17). However, the mechanisms involved in the assembly of SARS-CoV are not clear. Previous studies of mouse hepatitis virus (MHV), a serotype 2 coronavirus, indicated that both transmembrane envelope proteins E and M are essential for the assembly of virus particles (28). Coexpression of E and M proteins in cultured cells produced virus-like particles (VLPs) that are not infectious (28). In addition, the assembly of MHV genomic RNA is nucleocapsid independent (21), but binding of the N protein to a specific sequence, termed the packaging signal (PS), located near the 3' terminus of the open reading frame 1b in the viral genome facilitates assembly of the genomic RNA into virus particles (20, 22, 29). The length of PS required for the packaging of viral genome varies among coronaviruses. Results from bioinformatics analysis suggested a putative core PS (PS_{core}) of SARS-CoV with a size of about 70 nt (24). Nevertheless, the precise PS of SARS-CoV has not been biologically demonstrated, and whether the assembly of SARS-CoV is nucleocapsid dependent remains unclear.

In this study, we established a system to produce SARS-CoV

* Corresponding author. Mailing address: Institute of Biochemistry and Molecular Biology, National Taiwan University College of Medicine, No. 1, Jen-Ai Road, 1st Section, Taipei 100, Taiwan. Phone: 886 2 23123456, ext. 8217. Fax: 886 2 23915295. E-mail: mfchang@ntumc.org.

VLPs in Vero E6 cells. This VLP system is a valuable tool for studying the assembly, the tissue tropism, and the pathogenesis of SARS-CoV. We also identified the PS of SARS-CoV and found it to confer the packaging of heterologous green fluorescent protein (GFP)-PS mRNA in a nucleocapsid-dependent manner. Furthermore, two independent RNA-binding domains in the nucleocapsid protein of SARS-CoV were identified.

MATERIALS AND METHODS

Cell line and culture condition. Cells of the Vero E6 line (African green monkey kidney cells) were obtained from the Center for Disease Control of Taiwan. The cells were maintained at 37°C with 5% CO₂ in Dulbecco's modified Eagle's medium supplemented with 10% heat-inactivated fetal bovine serum (HyClone) plus 100 U of penicillin and 100 µg of streptomycin per ml.

Propagation of SARS-CoV (TW1 strain) and isolation of viral RNA. For virus propagation, Vero E6 cells were infected with SARS-CoV TW1 strain at 100 50% tissue culture infective doses. Three days postinfection, the culture medium was collected, and cell debris was clarified in a microcentrifuge for 1 min at 14,000 rpm. Virus particles in the supernatant were precipitated in 50% saturated ammonium sulfate at 4°C for 90 min, collected after centrifugation in a microcentrifuge at 8,000 rpm for 30 min, and resuspended in phosphate-buffered saline for further RNA extraction. Isolation of viral genomic RNA followed a single-step extraction method as described previously (2, 5).

Construction of plasmids. (i) **Plasmids pcDNA-E-V5HisTopo92, pcDNA-M-V5HisTopo158, pcDNA-N-V5HisTopo56, and pcDNA-S-V5HisTopo182.** Plasmids pcDNA-E-V5HisTopo92, pcDNA-M-V5HisTopo158, pcDNA-N-V5HisTopo56, and pcDNA-S-V5HisTopo182 represent the V5His-tagged small envelope, membrane, nucleocapsid, and spike protein, respectively, of SARS-CoV (TW1 strain; GenBank accession number AY291451) (11) and were generated by inserting individual cDNA fragments into pcDNA3.1/D/V5-His-TOPO (Invitrogen). The cDNA fragments were amplified by reverse transcriptase PCR from the genomic RNA with the following primer sets: KOZ26117F (caccATGTAC TCATTCGTTTCGGAAGAAACAGG; lowercase letters indicate extra sequences that are not derived from the genomic RNA but are added to the primer for cloning purposes) and 26344R (GACCAGCAAGATCAGGAAGCTCC) for the E protein; KOZ26398F (caccATGGCAGACAAACGGTACTATTACCG) and 27060R (CTGTACTAGCAAAGCAATATTGTCGTTGCTACCGGCGT) for the M protein; 28120EF (caccATGTCTGATAATGGACCCCAATCAAACCA ACGTAGTG) and 29385R (TGCTGAGTTGAATCAGCAGAAGCTCC) for the N protein; and KOZ21492mAgF (caccATGTTTATTTCCTATTATTCT TACTCTACTAGTGGTAGTGACCTTGACCGTTGCA) and 25256XR (ctc gagTGTGTAATGTAATTTGACACCCTTGAGAACTGGCTC) for the S protein of SARS-CoV.

(ii) **Plasmid pSec-S(14-1255)-Tag2A.** For generation of plasmid pSec-S(14-1255)-Tag2A, a cDNA fragment representing the spike protein of SARS-CoV from amino acid residues 14 to 1255 was amplified from the viral cDNA with the primer set 21531SF (cttagcggccagcggccagTGACCTTGA CCGTTGCACCA CTT) and 25256XR and cloned into the SfiI-XhoI sites of pSec-Tag2A (Invitrogen) after digestion with SfiI and XhoI restriction endonucleases. This plasmid encodes a MycHis-tagged fusion protein of the spike protein.

(iii) **Plasmids pCRII-TOPO-PS63, pCRII-TOPO-PS580, pEGFP-N1-PS63, and pEGFP-N1-PS580.** Plasmids pEGFP-N1-PS63 and pEGFP-N1-PS580 represent heterologous genes under the control of the cytomegalovirus promoter, with the putative package signal of SARS-CoV genomic RNA from nt 19888 to 19950 and nt 19715 to 20294, respectively, inserted into the 3' noncoding region of the GFP gene. These plasmids were derived from pCRII-TOPO-PS63 and pCRII-TOPO-PS580, respectively. Plasmid pCRII-TOPO-PS63 was generated by inserting a cDNA fragment amplified from the viral cDNA with primer set S-PKF (GCGGCCGAGAGTGCTTGTCTCACTACTGTC) and S-PKR (AAAGGTCTACCTGTCTCTCC) into pCRII-TOPO (Invitrogen). After treatment of plasmid pCRII-TOPO-PS63 with NotI restriction endonuclease, the resulting PS-containing fragment was inserted into the NotI site of pEGFP-N1 (Clontech) to generate pEGFP-N1-PS63. Generation of plasmids pCRII-TOPO-PS580 and pEGFP-N1-PS580 followed the procedures as described for pCRII-TOPO-PS63 and pEGFP-N1-PS63, respectively, except that the primer set used was 19715NF (GCGGCCGCTGAGCTTTGGGCTAAGCGTA) and 20294R (A AGACCGCAAGTTGTCCAT).

Transient transfection and production of SARS-CoV VLPs. Expression of SARS-CoV structural proteins was performed by infecting cells with recombi-

nant vaccinia virus (vTF7-3) harboring the T7 RNA polymerase gene (1), followed by DNA transfection with cationic liposomes (Invitrogen) as described previously (16, 32), with modifications. Briefly, 4×10^6 rapidly dividing Vero E6 cells in a 100-mm dish were infected with vTF7-3 at a multiplicity of infection of 0.0625. Two hours postinfection, expression plasmids were mixed with Lipofectin and added to the cells. At 6 to 8 h posttransfection, the DNA-Lipofectin complexes were removed, and 8 ml of Dulbecco's modified Eagle's medium containing 10% heat-inactivated fetal bovine serum was added. The transfected cells were incubated at 37°C for 2 days before harvest. For production of SARS-CoV VLPs with E, M, N, and S proteins, 6 µg of each of the structural protein-encoding plasmids pcDNA-E-V5HisTopo92, pcDNA-M-V5HisTopo158, pcDNA-N-V5HisTopo56, and pSec-S(14-1255)-Tag2A (or pcDNA-S-V5HisTopo182 if indicated) was used in the cotransfection experiments. Two days posttransfection, 5 ml of medium was added to the transfected cells, and incubation was continued for another 2 days before harvest of the VLPs. To examine the assembly of the packaging signal of SARS-CoV, 6 µg of either pEGFP-N1-PS63 or pEGFP-N1-PS580 was cotransfected with the four structural protein-encoding plasmids into the Vero E6 cells, generating VLP(GFP-PS63) and VLP(GFP-PS580), respectively. For generation of VLPdN, cotransfection experiments were performed with 6 µg of each of the S-, E-, and M-encoding plasmids and the PS plasmid pEGFP-N1-PS580.

Harvest and purification of SARS-CoV VLPs. Harvest and purification of SARS-CoV VLPs followed a previously described procedure (27), with modifications. Briefly, culture medium was harvested 4 days posttransfection and clarified by centrifugation at 3,000 rpm in an RA-4F rotor (Kubota) for 5 min. The supernatant was layered over a 20% sucrose buffer (20% sucrose, 20 mM HEPES, pH 7.4, 0.1% bovine serum albumin [BSA]) and centrifuged at 40,000 rpm in an SW41 rotor (Beckman) for 5 h at 4°C. VLPs collected in the pellet were resuspended in 100 µl of phosphate-buffered saline and stored at -80°C. For separation of various VLPs with different compositions, the virus suspension was further loaded on a discontinuous sucrose gradient consisting of 20, 30, 50, and 60% sucrose in 20 mM HEPES (pH 7.4) and 0.1% BSA and then centrifuged in the SW41 rotor at 26,700 rpm for 3.5 h at 4°C. Fractions containing VLPs with different compositions were analyzed for the presence of SARS-CoV structural proteins by Western blot analysis. The density of VLPs was determined by a refractometer (ATAGO).

Western blot analysis. To carry out Western blot analysis, protein lysates prepared from transfected cells and VLPs were resolved by 13% polyacrylamide gel electrophoresis and electrotransferred onto an Immobilon-P membrane (Millipore) as described previously (3). The V5His-tagged structural proteins of SARS-CoV were detected by using as the primary antibodies mouse monoclonal antibody against the V5 epitope (Invitrogen) and polyclonal antibodies that were generated by immunizing mice with SARS-CoV previously inactivated by ⁶⁰Co irradiation (10). GFP was detected with rabbit polyclonal antibodies against GFP provided by S.-L. Doong (National Taiwan University, Taipei, Taiwan). Specific interactions between antigens and antibodies were detected by the enhanced chemiluminescence system (ECL; Amersham Biosciences).

Purification of recombinant N proteins of SARS-CoV. Recombinant SARS-CoV N protein and its deletion mutants with a His tag at their N termini were expressed in *Escherichia coli* BL21(DE3) cells after induction with 1 mM isopropyl-β-D-thiogalactopyranoside. To prepare protein lysates, the bacterial cells were spun down and resuspended in lysis buffer consisting of 50 mM sodium phosphate, pH 8.0, 300 mM NaCl, 10 mM imidazole, and 6 M urea. After centrifugation, the supernatant was loaded onto a Ni-nitrilotriacetic acid affinity column (QIAGEN), and the His-tagged N proteins were recovered with elution buffer consisting of 50 mM sodium phosphate, pH 8.0, 300 mM NaCl, 250 mM imidazole, and 6 M urea. The eluate was dialyzed against 50 mM sodium phosphate buffer at pH 7.4 containing 150 mM NaCl, 1 mM EDTA, and 0.01% Na₃ and concentrated with an Amicon Ultra-15 concentrator (Millipore) before being loaded onto a fast-performance liquid chromatography (FPLC) system equipped with a HiLoad 16/60 Superdex-75 column (Pharmacia Bioscience). Fractions containing proteins of interest were pooled together for further studies.

FB assay. To examine the RNA-binding activity of the N protein of SARS-CoV, a filter binding (FB) assay was carried out as previously described (4, 9), with modifications. Briefly, the recombinant N proteins purified through FPLC were further dialyzed against FB buffer consisting of 20 mM HEPES-KOH, pH 7.5, 4 mM MgCl₂ and 40 mM KCl at 4°C overnight. To prepare RNA probe, plasmid pCRII-TOPO-PS580 was linearized with NheI restriction endonuclease and used as the template to perform in vitro transcription by T7 RNA polymerase in the presence of [α -³²P]UTP. This generated [α -³²P]UTP-labeled PS318 RNA representing SARS-CoV genomic RNA from nt 19715 to 20032. The PS318 RNA probe was dissolved in the FB buffer and heated at 70°C for 3 min

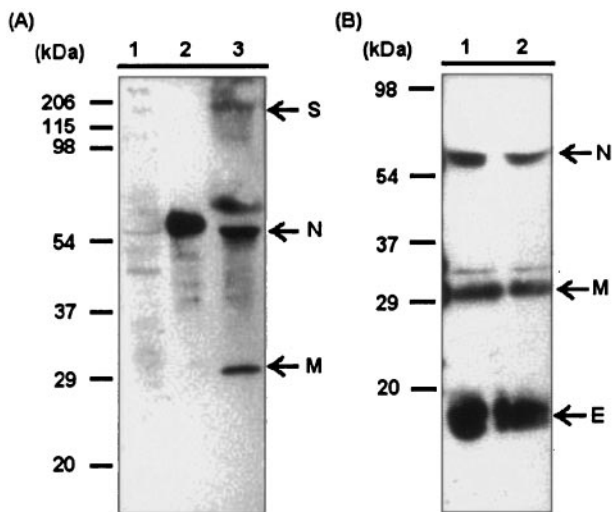


FIG. 1. Analysis of structural proteins that are assembled into SARS-CoV VLPs. Vero E6 cells previously infected with recombinant vaccinia virus vTF7-3 were cotransfected with plasmids pSec-S(14-1255)-Tag2A, pcDNA-E-V5HisTopo92, pcDNA-M-V5HisTopo158, and pcDNA-N-V5HisTopo56 encoding MycHis-tagged S and V5His-tagged E, M, and N structural proteins, respectively, of SARS-CoV. Four days posttransfection, culture medium was collected, and VLPs were isolated after 20% sucrose cushion centrifugation. Structural proteins assembled into the VLPs were detected by Western blot analysis with mouse polyclonal antibodies generated with ^{60}Co -inactivated SARS-CoV (A) and mouse monoclonal antibody against the V5 epitope of the V5His-tagged structural proteins N, M, and E (B). Lanes 1 and 2 in panel A represent protein lysates of untransfected Vero E6 cells and Vero E6 cells transfected with N-encoding plasmid as negative and positive controls, respectively. Lanes 1 and 2 in panel B represent duplicate experiments.

and then at 37°C for 15 min. Meanwhile, individual N protein was preincubated at 37°C for 15 min and then mixed with the preheated RNA probe (10,000 cpm/ μl). After incubation at 37°C for another 10 min, the reaction mixtures were passed through prewetted nitrocellulose filters (0.45- μm pore size). The filters were then washed in ice-cold FB buffer and air dried. RNA-binding activities of the N proteins were detected by autoradiography. In addition, to determine the binding specificity, various amounts of nonlabeled specific (PS318) and nonspecific (hepatitis C virus [HCV] NCR341) RNA competitors were mixed individually with the labeled PS318 RNA probe before incubating with the N proteins. The HCV NCR341 RNA represents HCV genomic RNA from nt 1 to 341 and was synthesized *in vitro* by T7 RNA polymerase as previously described (31).

RESULTS

Expression of the structural proteins of SARS-CoV in Vero E6 cells and production of SARS-CoV VLPs. For examination of the assembly of SARS-CoV, a culture system that expresses the viral structural proteins and produces SARS-CoV VLPs was established. The experiments were performed initially by cotransfecting Vero E6 cells with plasmids that encode a MycHis-tagged S protein and V5His-tagged E, M, and N proteins of SARS-CoV. Four days posttransfection, culture medium was collected and subjected to isolation of VLPs by sucrose cushion centrifugation. Structural proteins assembled into the VLPs were examined by Western blot analysis with mouse hyperimmune serum induced by ^{60}Co -inactivated SARS-CoV and with mouse monoclonal antibody against the V5 epitope of the V5His-tagged structural proteins. As shown in Fig. 1A, the mouse hyperimmune serum detected the structural proteins S, M, and N in the SARS-

CoV VLPs but not the E protein (lane 3). This was possibly due to the lack of any or the presence of only a few antibodies specific to the E protein in the mouse hyperimmune serum. When anti-V5 epitope antibody was applied, the V5His-tagged fusion proteins N, M, and E were successfully detected (Fig. 1B). We have recently detected SARS-CoV VLPs consisting of S, E, and M proteins under electron microscopy (data not shown). To determine whether S and N proteins are required in forming SARS-CoV VLPs, cotransfection experiments were performed with the plasmids encoding the V5His-tagged E and M proteins in the presence or absence of V5His-tagged S- and N-encoding plasmids. The culture medium was collected 4 days posttransfection and subjected to sucrose cushion centrifugation and Western blot analysis. In the absence of S and N proteins, both E and M proteins expressed in Vero E6 cells were detected in the culture medium (Fig. 2A). Vero E6 cells were then transfected individually with the E-encoding and M-encoding plasmids. Following a sucrose cushion centrifugation, the pellets were further purified on a discontinuous sucrose gradient. Western blot analysis demonstrated that both E and M proteins could be released into the culture medium when each was expressed alone (Fig. 2B). The M protein was mainly detected in fractions 4 to 9 (density, 1.081 to 1.228 g/cm^3), whereas the E protein was detected in fractions 1 to 6 (density, 1.008 to 1.128 g/cm^3). The distribution of M protein was shifted to fractions 3 to 6, with density ranging from 1.067 to 1.113 g/cm^3 when the M protein was coexpressed with the E protein. It is likely that E and M proteins form VLPs when they are coexpressed. However, previous studies demonstrated that E proteins of MHV and infectious bronchitis virus could be released into medium as vesicles when it was expressed alone (6, 18). Whether the sedimentable particles of E and of M represent formation of SARS-CoV VLPs or formation of the viral protein vesicles is not clear. Different forms of SARS-CoV VLPs produced in the presence of all four structural proteins were examined following a discontinuous sucrose gradient (Fig. 2C). Fractions 5 and 6 likely represent VLPs that contain the viral E and M proteins with densities of about 1.097 and 1.116 g/cm^3 , respectively. Fraction 7 contained the majority of SARS-CoV VLPs that bear the four structural proteins with a density of around 1.132 g/cm^3 .

Packaging of SARS-CoV RNA required sequences beyond the 63-nt putative PS_{core}. It was previously demonstrated that binding of the MHV N protein to the PS located near the 3' terminus of the open reading frame 1b facilitates the assembly of viral genomic RNA (20, 22, 29). The PS_{core} of MHV was mapped to a stem-loop structure consisting of 69 nt, but a 190-nt PS_{core}-containing RNA has a much higher packaging activity (22). The PS of SARS-CoV has been predicted by bioinformatics analysis (24) but not yet functionally defined. In this study, secondary structure analysis by the Mfold program revealed a distinct stem-loop structure that remains conserved in the 63-nt putative PS_{core} (PS63) RNA of SARS-CoV and the PS_{core}-containing PS580 RNA (Fig. 3). PS63 and PS580 RNA represent SARS-CoV genomic RNA from nt 19888 to 19950 and nt 19715 to 20294, respectively. To establish a culture system in which the packaging activities of PS63 and PS580 RNA can be easily followed, plasmids pEGFP-N1-PS63 and pEGFP-N1-PS580 that represent heterologous mRNAs GFP-PS63 and GFP-PS580 consisting of PS63 and PS580, respectively, inserted into the 3' noncoding region of GFP re-

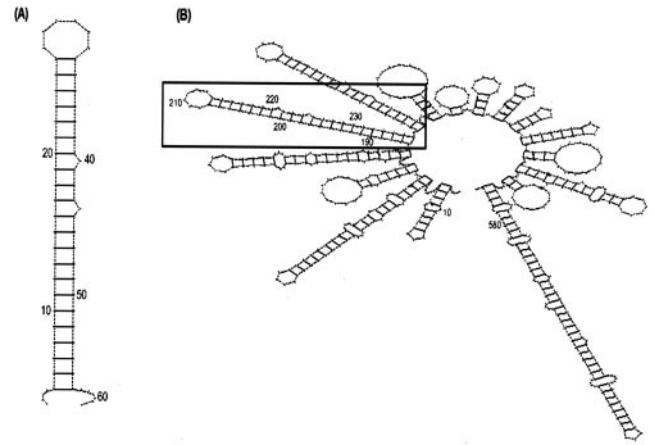
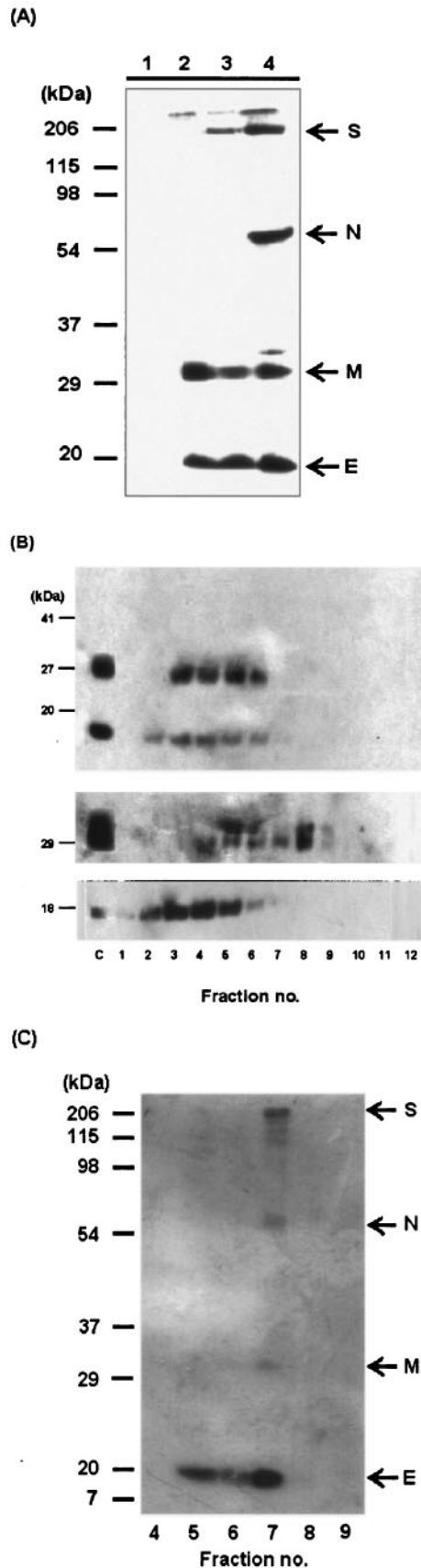


FIG. 3. Secondary structures of the SARS-CoV putative packaging signal PS63 and PS580 RNA. The Mfold program was used to predict the secondary structures of SARS-CoV PS_{core} PS63 RNA encompassing the viral genomic RNA from nt 19888 to 19950 (A) and the PS_{core}-containing PS580 RNA from nt 19715 to 20294 (B). The black rectangle in panel B marks the unique stem-loop structure of the PS_{core} that remains conserved in the PS580 RNA.

porter were generated and transiently transfected into Vero E6 cells. Two days posttransfection, the green fluorescence of GFP was detected by fluorescence microscopy, indicating that GFP-PS63 and GFP-PS580 RNA can be expressed in the transfected cells (Fig. 4). Assembly of the viral genomic RNAs was then examined by transfecting Vero E6 cells with plasmids encoding the viral structural proteins S, E, M, and N and one of the packaging signal plasmids, pEGFP-N1-PS63 and pEGFP-N1-PS580. Four days posttransfection, VLPs were isolated from the culture medium. The VLP produced from cells cotransfected with pEGFP-N1-PS63 was tentatively named VLP(GFP-PS63), whereas that from cells transfected with

FIG. 2. Purification and analysis of SARS-CoV VLPs. (A) E and M proteins could be released from transfected Vero E6 cells in the absence of S and N proteins. To examine the requirements for the formation of SARS-CoV VLPs, Vero E6 cells previously infected with recombinant vaccinia virus vTF7-3 were cotransfected with plasmids encoding the V5His-tagged E and M proteins (lane 2); E, M, and S proteins (lane 3); or E, M, S, and N proteins (lane 4). Culture medium collected 4 days posttransfection was subjected to a 20% sucrose cushion centrifugation and Western blot analysis with the mouse monoclonal antibody against the V5 epitope. Lane 1 represents the nontransfected control. (B) Both E and M proteins could be released into the culture medium when each was expressed alone. Culture medium was collected from Vero E6 cells transfected with plasmids encoding E and M (upper panel), M (middle panel), or E (lower panel). Following a sucrose cushion centrifugation, the pellets were further purified on a discontinuous sucrose gradient as described in Materials and Methods. Fractions were collected and subjected to Western blot analysis. Lanes C represent protein lysates of transfected cells and were used as positive controls. (C) Analysis of different forms of SARS-CoV VLPs. SARS-CoV VLPs formed in the presence of all four structural proteins as demonstrated in panel A (lane 4) were further purified through a discontinuous sucrose gradient. Fractions 4 to 9 were analyzed by Western blot analysis with the V5 epitope-specific antibody for the presence of SARS-CoV structural proteins. Fraction 7 contained the majority of SARS-CoV VLPs, which consisted of all four structural proteins and had a density of around 1.132 g/cm³.

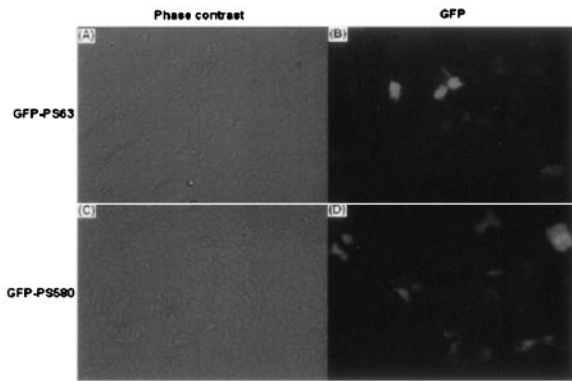


FIG. 4. Expression of pEGFP-N1-PS63 and pEGFP-N1-PS580 in Vero E6 cells. Vero E6 cells were transfected individually with pEGFP-N1-PS63 (panels A and B) and pEGFP-N1-PS580 (panels C and D) bearing 63 and 580 nt, respectively, of the putative packaging signals of SARS-CoV inserted into the 3' noncoding region of the GFP gene. Two days posttransfection, green fluorescence of GFP in the transfected cells was visualized by fluorescence microscopy (panels B and D). Panels A and C show the phase contrast images of the transfected cells.

pEGFP-N1-PS580 was named VLP(GFP-PS580). Western blot analysis demonstrated that the structural proteins of SARS-CoV can be assembled into both VLP(GFP-PS63) and VLP(GFP-PS580) (Fig. 5A). In addition, GFP was detected only in the transfected cells but not in the VLPs (Fig. 5B).

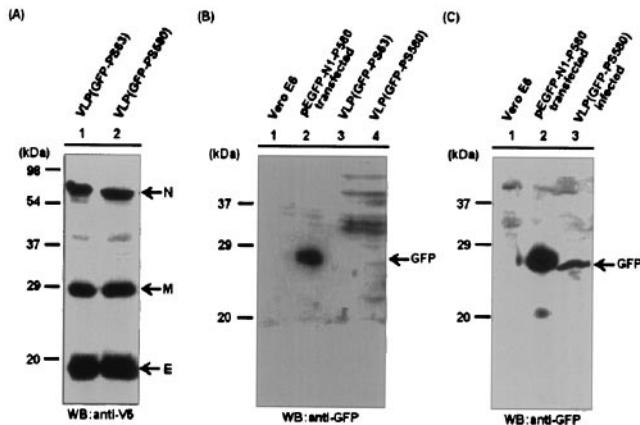


FIG. 5. Expression of GFP in VLP(GFP-PS580)-infected Vero E6 cells. Plasmid pEGFP-N1-PS63 or pEGFP-N1-PS580 was transfected into Vero E6 cells together with plasmids pSec-S(14-1255)-Tag2A, pcDNA-E-V5HisTopo92, pcDNA-M-V5HisTopo158, and pcDNA-N-V5HisTopo56 that encode a MycHis-tagged S and V5His-tagged E, M, and N structural proteins of SARS-CoV, respectively. Four days posttransfection, VLPs were harvested from the culture medium, partially purified, and used to infect Vero E6 cells to examine the infectivity of the VLPs and the packaging activity of the PS RNAs. The viral proteins that were assembled into the VLPs, VLP(GFP-PS63) and VLP(GFP-PS580), were examined by Western blot analysis with anti-V5 antibody (panel A). Expression of GFP in the VLP(GFP-PS580)-infected cells was examined with anti-GFP antibodies 2 days postinfection (panel C, lane 3). Whether GFP was simultaneously incorporated into the VLPs was also examined (panel B, lanes 3 and 4). Cell lysates prepared from untreated Vero E6 cells (panels B and C, lanes 1) and pEGFP-N1-PS580-transfected cells (panels B and C, lanes 2) were used as negative and positive controls, respectively.

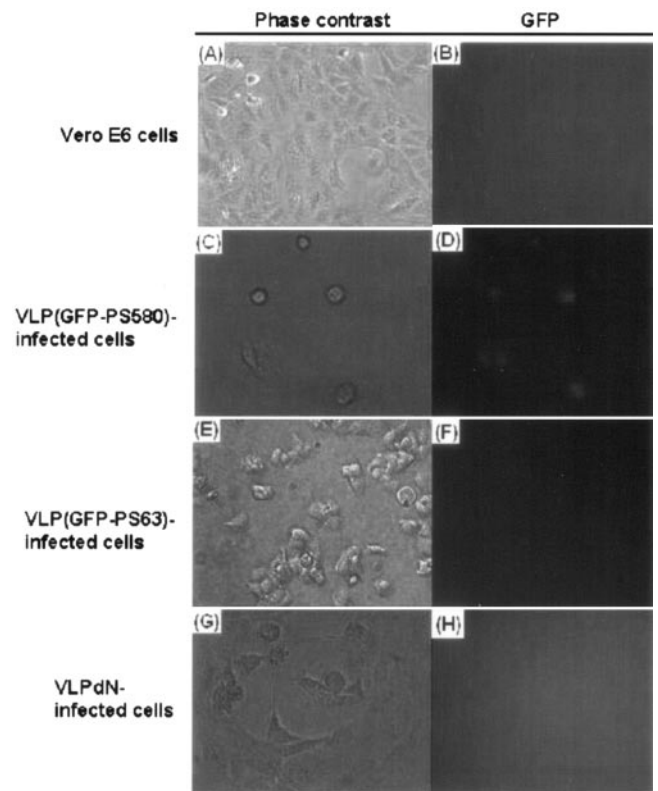
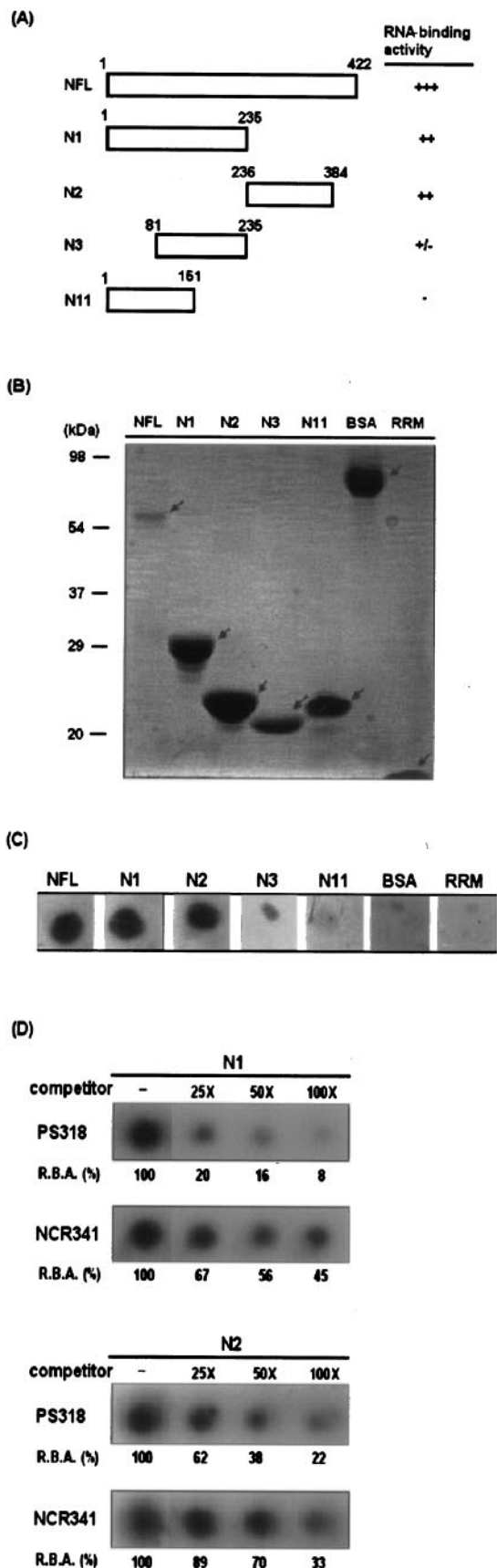


FIG. 6. Packaging of GFP-PS heterologous mRNA into VLPs required sequences beyond the putative 63-nt PS_{core} and was nucleocapsid dependent. Vero E6 cells were infected with either VLP(GFP-PS580) (panels C and D) or VLP(GFP-PS63) (panels E and F). Two days postinfection, green fluorescence in VLP(GFP-PS580)-infected cells was detected by fluorescence microscopy. Panels G and H represent Vero E6 cells that were infected with VLPdN. Untreated Vero E6 cells are shown as negative controls (panels A and B).

These results indicate that GFP expressed in the transfected cells is not copackaged into the VLPs and that the VLPs purified from culture medium are not contaminated with GFP. Whether the GFP-PS63 and GFP-PS580 RNA had been packaged into the VLPs was determined by infecting Vero E6 cells with VLP(GFP-PS63) and VLP(GFP-PS580), respectively, and examining GFP expression in the infected cells. As shown in Fig. 6, green fluorescence of GFP in Vero E6 cells was detected by fluorescence microscopy 2 days posttransfection of the VLP(GFP-PS580) (Fig. 6D) but not in the cells infected with VLP(GFP-PS63) (Fig. 6F). However, the green fluorescence signal in VLP(GFP-PS580)-infected cells was low. This was probably due to the low copy number of GFP mRNA assembled into the VLPs, which may have been limited to one or only a few copies. To further confirm the packaging activity of the GFP-PS580 RNA, Western blot analysis was performed with antibodies specific to the GFP. These results clearly demonstrated expression of GFP in VLP(GFP-PS580)-infected cells (Fig. 5C) but not in the VLP(GFP-PS63)-infected cells (data not shown). Taken together, these results indicate that the PS_{core}-containing PS580 RNA bears a functional packaging signal of SARS-CoV important for the assembly of the viral RNA into VLPs.



Packaging of GFP-PS heterologous mRNA into SARS-CoV VLPs is nucleocapsid dependent. Previous study showed that MHV VLPs could be assembled in a nucleocapsid-independent manner and that viral RNA could be packaged in the absence of the viral N protein (20, 28). To determine whether the N protein of SARS-CoV is dispensable in the packaging of the viral RNA, Vero E6 cells were cotransfected with the packaging signal plasmid pEGFP-N1-PS580 and the expressing plasmids encoding the viral structural proteins, S, E, and M in parallel with a control experiment that included the N-encoding plasmid. VLPdN that lacks the N protein was harvested from the culture medium of transfected cells and used to infect Vero E6 cells. Two days postinfection, green fluorescence was detected in VLP(GFP-PS580)-infected cells (Fig. 6D) but not in VLPdN-infected cells (Fig. 6H). These results indicate that the assembly of SARS-CoV RNA is nucleocapsid dependent.

Two independent RNA-binding domains in the viral N protein specifically bind to SARS-CoV RNA. To investigate the RNA-binding characteristics of the N protein of SARS-CoV, PS318 RNA representing SARS-CoV genomic RNA from nt 19715 to 20032 was transcribed in vitro in the presence of [α - 32 P]UTP. As predicted by the Mfold program, PS318 RNA possesses the conserved stem-loop structure of the 63-nt PS_{core} (PS63) RNA (data not shown). The [α - 32 P]UTP-labeled PS318 RNA was used as the probe to perform a filter binding assay with FPLC-purified recombinant N proteins of SARS-CoV. BSA and a putative RNA recognition motif (RRM) of the eIF3 subunit p116 (M.-F. Chang et al., unpublished data) were used as controls. As shown in Fig. 7, both N1 and N2 that represent the N-terminal 235 amino acid residues of the N protein and the C-terminal domain from amino acid residues 236 to 384, respectively, were capable of interacting with PS318 RNA, but the control proteins had no binding activity. The RNA-binding activity of the N-terminal domain was significantly diminished when deletions were generated that removed the N protein amino acid sequences from 1 to 80 (N3) or from 152 to 235 (N11). Specificity of the RNA-binding activity of the N protein was further examined by RNA competition analysis. Various amounts of nonlabeled specific competitor (PS318 RNA) and nonspecific competitor (HCV NCR341 RNA) were added to the reaction mixtures of the [α - 32 P]UTP-labeled PS318 RNA and the N1 or N2 protein in the filter binding

FIG. 7. The RNA-binding activity of the full-length SARS-CoV N protein and its deletion mutants. (A) Schematic representation of the recombinant N proteins and their relative binding activities to PS318 RNA. (B) Coomassie blue staining of the purified N proteins used in the FB assay. BSA and a putative RRM of the eIF3 subunit p116 were used as controls. (C) The FB assay was performed with [α - 32 P]UTP-labeled PS318 RNA and 40 ng each of the purified N proteins, BSA, and RRM. (D) Specificity of the RNA-binding activity of the N protein subdomains N1 and N2. For determination of the binding specificity of the N1 and N2 subdomains to SARS-CoV PS318 RNA, various amounts of nonlabeled specific competitor (PS318 RNA) and nonspecific competitor (HCV NCR341 RNA) as indicated were mixed with [α - 32 P]UTP-labeled PS318 RNA before addition of the purified N1 and N2 proteins. Autoradiograms are shown. Relative binding activities (RBA) of the N1 and N2 proteins to the PS318 RNA in the presence of competitors were calculated by normalization of the intensities of signals in each set to that without competitors.

assay. At a 25-fold molar excess of specific competitor, the relative RNA-binding activities of the N1 and N2 proteins were decreased to 20% and 62%, respectively, values much lower than those obtained with the nonspecific competitor (Fig. 7). We conclude that there are two RNA-binding sites in the N protein of SARS-CoV, the N-terminal domain from amino acid residues 1 to 235 and the C-terminal domain from amino acid residues 236 to 384.

DISCUSSION

In this study, we found that SARS-CoV structural proteins S, E, M, and N expressed in Vero E6 cells could form VLPs that were subsequently released into the culture medium. The E and M proteins are likely to form SARS-CoV VLPs when they are coexpressed. In addition, both E and M expressed alone were capable of forming sedimentable particles and released from transfected cells. Packaging of viral RNA into VLPs required the viral N protein and a packaging signal within a domain from nt 19715 to 20294 of the genomic RNA. Two RNA-binding domains of the N protein specific to SARS-CoV RNA were identified.

In MHV, M protein is the most abundant transmembrane envelope glycoprotein in the virus particles and infected cells, whereas E protein is present only in a minute amount (8). However, we found that in some cases, the amounts of E protein in different forms of SARS-CoV VLPs were equivalent or even higher than the amounts of M protein (Fig. 2A). This may be partially explained by the fact that the SARS-CoV E protein can be released from cells when it is expressed alone (Fig. 2B), similar to the E proteins of MHV and infectious bronchitis virus (6, 18). However, it is interesting that the E and M proteins were detected in several fractions in the absence of the viral S and N proteins (Fig. 2B), whereas SARS-CoV VLPs containing S, E, M, and N were detected in a single fraction (Fig. 2C).

Packaging signals are defined as the *cis*-acting sequences required for efficient packaging of the genomic RNA during virus assembly. As predicted by the Mfold program, the putative PS_{core} of SARS-CoV possesses a stem-loop structure that remains conserved in the PS_{core}-containing PS580 RNA (Fig. 3). Nevertheless, green fluorescence of GFP can only be detected in VLP(GFP-PS580)-infected but not the VLP(GFP-PS63)-infected cells (Fig. 6D and F), indicating that packaging of viral RNA requires sequences beyond the stable stem-loop structure. In contrast to MHV, which is capable of packaging viral RNA in the absence of N protein, the assembly of GFP-PS RNA into SARS-CoV VLPs is nucleocapsid dependent (Fig. 6H). The successful utilization of GFP as a tracker for the packaging of SARS-CoV RNA implies a possible application in generating other heterologous mRNAs that contain the SARS-CoV packaging signal. The heterologous mRNAs would be packaged into SARS-CoV VLPs and expressed upon infection of specific human tissues by these VLPs. Thus, the SARS-CoV VLPs could be used as a tissue-specific viral vector for gene therapy or drug delivery.

By performing a filter binding assay with the PS_{core}-containing PS318 RNA and FPLC-purified recombinant N proteins of SARS-CoV, we identified two independent RNA-binding domains of the N protein located each in the N-terminal and the

C-terminal domains (Fig. 7). Deletion in the region from amino acid residues 1 to 80 (N3 mutant) or 152 to 235 (N11 mutant) significantly diminished the RNA-binding activity of the N-terminal domain. These results are consistent with nuclear magnetic resonance studies indicating that the N-terminal domain from amino acid residues 49 to 178 of the nucleocapsid protein possesses RNA-binding activity (12). Our preliminary studies also demonstrated that the N protein consists of two structurally independent domains (T.-H. Huang et al., unpublished data). The deletion from amino acid residues 1 to 80 or 152 to 235 both resulted in disruption of the structure of the N-terminal domain from amino acid residues 49 to 178. Taken together, these results indicate that the N-terminal structure is essential for the RNA-binding activity of the N-terminal domain. Serial deletion analysis in both the N-terminal and the C-terminal domain would reveal the minimal sequences required for the RNA-binding activity of the nucleocapsid protein. Furthermore, cotransfection experiments may be performed to determine whether PS318 RNA can interact with the nucleocapsid protein in Vero E6 cells and, as PS580 RNA does, form infectious VLPs in the presence of other structural proteins.

Although viral particles of SARS-CoV have been detected in tissues such as lung of infected patients (23), the cell types that are most susceptible to SARS-CoV infection in patients are not fully understood. Using mouse polyclonal antibodies against ⁶⁰Co-inactivated SARS-CoV generated in our laboratory, we have detected viral proteins in type II pneumocytes of SARS patients (10). Angiotensin-converting enzyme 2 was previously proposed to be a receptor of SARS-CoV (17). A recent study also demonstrated that CD209L (L-SIGN) could be a receptor of SARS-CoV on type II pneumocytes (13). Nevertheless, the mechanism by which SARS-CoV causes SARS remains unclear. The VLPs generated in this study may be used to safely study the tissue tropisms and pathogenesis of SARS-CoV.

ACKNOWLEDGMENTS

We gratefully acknowledge C.-L. Kao for providing SARS-CoV-infected Vero E6 cells, C.-L. Liao for the recombinant vaccinia virus vTF7-3, and S.-L. Doong for the anti-GFP polyclonal antibodies. We also thank M. Evans for critical reading of the manuscript and S.-C. Wu and Y.-H. Lai for helping prepare the figures.

This work was supported by research grants NSC92-3112-B-002-029 and NSC93-2751-B-002-003-Y to M.-F. Chang, by grant NSC92-2751-B-001-020-Y to T.-H. Huang from the National Science Council of the Republic of China, and by a grant from the Ministry of Education, Taiwan, to the Center for Genomic Medicine of National Taiwan University.

REFERENCES

1. Belsham, G. J., J. K. Brangwyn, M. D. Ryan, C. C. Abrams, and A. M. King. 1990. Intracellular expression and processing of foot-and-mouth disease virus capsid precursors using vaccinia virus vectors: influence of the L protease. *Virology* **176**:524–530.
2. Chang, M. F., C. J. Chen, and S. C. Chang. 1994. Mutational analysis of delta antigen: effect on assembly and replication of hepatitis delta virus. *J. Virol.* **68**:646–653.
3. Chang, M. F., C. Y. Sun, C. J. Chen, and S. C. Chang. 1993. Functional motifs of delta antigen essential for RNA binding and replication of hepatitis delta virus. *J. Virol.* **67**:2529–2536.
4. Chang, S. C., J. C. Cheng, Y. H. Kou, C. H. Kao, C. H. Chiu, H. Y. Wu, and M. F. Chang. 2000. Roles of the AX₄GKS and arginine-rich motifs of hepatitis C virus RNA helicase in ATP- and viral RNA-binding activity. *J. Virol.* **74**:9732–9737.

5. Chomczynski, P., and N. Sacchi. 1987. Single-step method of RNA isolation by acid guanidinium thiocyanate-phenol-chloroform extraction. *Anal. Biochem.* **162**:156–159.
6. Corse, E., and C. E. Machamer. 2000. Infectious bronchitis virus E protein is targeted to the Golgi complex and directs release of virus-like particles. *J. Virol.* **74**:4319–4326.
7. Drosten, C., S. Gunther, W. Preiser, S. van der Werf, H. R. Brodt, S. Becker, H. Rabenau, M. Panning, L. Kolesnikova, R. A. Fouchier, A. Berger, A. M. Burguiera, J. Cinatl, M. Eickmann, N. Escricu, K. Grywna, S. Kramme, J. C. Manuguerra, S. Muller, V. Rickerts, M. Sturmer, S. Vieth, H. D. Klenk, A. D. Osterhaus, H. Schmitz, and H. W. Doerr. 2003. Identification of a novel coronavirus in patients with severe acute respiratory syndrome. *N. Engl. J. Med.* **348**:1967–1976.
8. Fischer, F., C. F. Stegen, P. S. Masters, and W. A. Samsonoff. 1998. Analysis of constructed E gene mutants of mouse hepatitis virus confirms a pivotal role for E protein in coronavirus assembly. *J. Virol.* **72**:7885–7894.
9. Gwack, Y., D. W. Kim, J. H. Han, and J. Choe. 1996. Characterization of RNA binding activity and RNA helicase activity of the hepatitis C virus NS3 protein. *Biochem. Biophys. Res. Commun.* **225**:654–659.
10. Hsiao, C. H., M. F. Chang, P. R. Hsueh, and I. J. Su. 2005. Immunohistochemical study of severe acute respiratory syndrome-associated coronavirus in tissue sections of patients. *J. Formos. Med. Assoc.* **104**:149–155.
11. Hsueh, P. R., C. H. Hsiao, S. H. Yeh, W. K. Wang, P. J. Chen, J. T. Wang, S. C. Chang, C. L. Kao, P. C. Yang, and SARS Research Group of NTU and NTUH. 2003. Microbiologic characteristics, serologic responses, and clinical manifestations in severe acute respiratory syndrome, Taiwan. *Emerg. Infect. Dis.* **9**:1163–1167.
12. Huang, Q., L. Yu, A. M. Petros, A. Gunasekera, Z. Liu, N. Xu, P. Hajduk, J. Mack, S. W. Fesik, and E. T. Olejniczak. 2004. Structure of the N-terminal RNA-binding domain of the SARS-CoV nucleocapsid protein. *Biochemistry* **43**:6059–6063.
13. Jeffers, S. A., S. M. Tusell, L. Gillim-Ross, E. M. Hemmila, J. E. Achenbach, G. J. Babcock, W. D. Thomas, Jr., L. B. Thackray, M. D. Young, R. J. Mason, D. M. Ambrosino, D. E. Wentworth, J. C. Demartini, K. V. Holmes. 2004. CD209L (L-SIGN) is a receptor for severe acute respiratory syndrome coronavirus. *Proc. Natl. Acad. Sci. USA* **101**:15748–15753.
14. Ksiazek, T. G., D. Erdman, C. S. Goldsmith, S. R. Zaki, T. Peret, S. Emery, S. Tong, C. Urbani, J. A. Comer, W. Lim, P. E. Rollin, S. F. Dowell, A. E. Ling, C. D. Humphrey, W. J. Shieh, J. Guarner, C. D. Paddock, P. Rota, B. Fields, J. DeRisi, J. Y. Yang, N. Cox, J. M. Hughes, J. W. LeDuc, W. J. Bellini, L. J. Anderson, and SARS Working Group. 2003. A novel coronavirus associated with severe acute respiratory syndrome. *N. Engl. J. Med.* **348**:1953–1966.
15. Lee, N., D. Hui, A. Wu, P. Chan, P. Cameron, G. M. Joynt, A. Ahuja, M. Y. Yung, C. B. Leung, K. F. To, S. F. Lui, C. C. Szeto, S. Chung, and J. J. Sung. 2003. A major outbreak of severe acute respiratory syndrome in Hong Kong. *N. Engl. J. Med.* **348**:1986–1994.
16. Lewis, T., and S. M. Matsui. 1996. Astrovirus ribosomal frameshifting in an infection-transfection transient expression system. *J. Virol.* **70**:2869–2875.
17. Li, W., M. J. Moore, N. Vasilieva, J. Sui, S. K. Wong, M. A. Berne, M. Somasundaran, J. L. Sullivan, K. Luzuriaga, T. C. Greenough, H. Choe, and M. Farzan. 2003. Angiotensin-converting enzyme 2 is a functional receptor for the SARS coronavirus. *Nature* **426**:450–454.
18. Maeda, J., A. Maeda, and S. Makino. 1999. Release of coronavirus E protein in membrane vesicles from virus-infected cells and E protein-expressing cells. *Virology* **263**:265–272.
19. Marra, M. A., S. J. Jones, C. R. Astell, R. A. Holt, A. Brooks-Wilson, Y. S. Butterfield, J. Khattri, J. K. Asano, S. A. Barber, S. Y. Chan, A. Cloutier, S. M. Coughlin, D. Freeman, N. Girn, O. L. Griffith, S. R. Leach, M. Mayo, H. McDonald, S. B. Montgomery, P. K. Pandoh, A. S. Petrescu, A. G. Robertson, J. E. Schein, A. Siddiqui, D. E. Smailus, J. M. Stott, G. S. Yang, F. Plummer, A. Andonov, H. Artsob, N. Bastien, K. Bernard, T. F. Booth, D. Bowness, M. Czub, M. Drebot, L. Fernando, R. Flick, M. Garbutt, M. Gray, A. Grolla, S. Jones, H. Feldmann, A. Meyers, A. Kabani, Y. Li, S. Normand, U. Stroher, G. A. Tipples, S. Tyler, R. Vogrig, D. Ward, B. Watson, R. C. Brunham, M. Krajden, M. Petric, D. M. Skowronski, C. Upton, R. L. Roper, and S. J. M. Jones. 2003. The genome sequence of the SARS-associated coronavirus. *Science* **300**:1399–1404.
20. Narayanan, K., C. J. Chen, J. Maeda, and S. Makino. 2003. Nucleocapsid-independent specific viral RNA packaging via viral envelope protein and viral RNA signal. *J. Virol.* **77**:2922–2927.
21. Narayanan, K., A. Maeda, J. Maeda, and S. Makino. 2000. Characterization of the coronavirus M protein and nucleocapsid interaction in infected cells. *J. Virol.* **74**:8127–8134.
22. Narayanan, K., and S. Makino. 2001. Cooperation of an RNA packaging signal and a viral envelope protein in coronavirus RNA packaging. *J. Virol.* **75**:9059–9067.
23. Nicholls, J. M., L. L. Poon, K. C. Lee, W. F. Ng, S. T. Lai, C. Y. Leung, C. M. Chu, P. K. Hui, K. L. Mak, W. Lim, K. W. Yan, K. H. Chan, N. C. Tsang, Y. Guan, K. Y. Yuen, and J. S. Peiris. 2003. Lung pathology of fatal severe acute respiratory syndrome. *Lancet* **361**:1773–1778.
24. Qin, L., B. Xiong, C. Luo, Z. M. Guo, P. Hao, J. Su, P. Nan, Y. Feng, Y. X. Shi, X. J. Yu, X. M. Luo, K. X. Chen, X. Shen, J. H. Shen, J. P. Zou, G. P. Zhao, T. L. Shi, W. Z. He, Y. Zhong, H. L. Jiang, and Y. X. Li. 2003. Identification of probable genomic packaging signal sequence from SARS-CoV genome by bioinformatics analysis. *Acta Pharmacol. Sin.* **24**:489–496.
25. Rota, P. A., M. S. Oberste, S. S. Monroe, W. A. Nix, R. Campagnoli, J. P. Icenogle, S. Penaranda, B. Bankamp, K. Maher, M. H. Chen, S. Tong, A. Tamin, L. Lowe, M. Frace, J. L. DeRisi, Q. Chen, D. Wang, D. D. Erdman, T. C. T. Peret, C. Burns, T. G. Ksiazek, P. E. Rollan, A. Sanchez, S. Liffick, B. Holloway, J. Limor, K. McCaustland, M. Olsen-Rasmussen, R. Fouchier, S. Gunther, A. D. M. E. Osterhaus, C. Drosten, M. A. Pallansch, L. J. Anderson, and W. J. Bellini. 2003. Characterization of a novel coronavirus associated with severe acute respiratory syndrome. *Science* **300**:1394–1399.
26. Stadler, K., V. Masighani, M. Eickmann, S. Becker, S. Abrignani, H. D. Klenk, and R. Rappuoli. 2003. SARS—beginning to understand a new virus. *Nat. Rev. Microbiol.* **1**:209–218.
27. Tsai, C. W., S. C. Chang, and M. F. Chang. 1999. A 12-amino-acid stretch in the hypervariable region of the spike protein S1 subunit is critical for cell fusion activity of mouse hepatitis virus. *J. Biol. Chem.* **274**:26085–26090.
28. Vennema, H., G. J. Godeke, J. W. Rossen, W. F. Voorhout, M. C. Horzinek, D. J. Opstelten, and P. J. Rottier. 1996. Nucleocapsid-independent assembly of coronavirus-like particles by co-expression of viral envelope protein genes. *EMBO J.* **15**:2020–2028.
29. Woo, K., M. Joo, K. Narayanan, K. H. Kim, and S. Makino. 1997. Murine coronavirus packaging signal confers packaging to nonviral RNA. *J. Virol.* **71**:824–827.
30. World Health Organization. 2004. World health report 2004—changing history. [Online.] <http://www.who.int/whr/2004/chapter5/en/>.
31. Yen, J. H., S. C. Chang, C. R. Hu, S. C. Chu, S. S. Lin, Y. S. Hsieh, and M. F. Chang. 1995. Cellular proteins specifically bind to the 5′-noncoding region of hepatitis C virus RNA. *Virology* **208**:723–732.
32. Yu, C. J., Y. C. Chen, C. H. Hsiao, T. C. Kuo, S. C. Chang, C. Y. Lu, W. C. Wei, C. H. Lee, L. M. Huang, M. F. Chang, H. N. Ho, and F. J. S. Lee. 2004. Identification of a novel protein 3a from severe acute respiratory syndrome coronavirus. *FEBS Lett.* **565**:111–116.